Pseudopotential theoretical study of the alkali metals under arbitrary pressure: Density, bulk modulus, and shear moduli

Daniel J. Rasky* and Frederick Milstein
University of California, Santa Barbara, California 93106
(Received 28 January 1985; revised manuscript received 9 September 1985)

Milstein and Hill previously derived formulas for computing the bulk and shear moduli, κ, μ, and μ', at arbitrary pressures, for cubic crystals in which interatomic interaction energies are modeled by pairwise functions, and they carried out the moduli computations using the complete family of Morse functions. The present study extends their work to a pseudopotential description of atomic binding. Specifically: (1) General formulas are derived for determining these moduli under hydrostatic loading within the framework of a pseudopotential model. (2) A two-parameter pseudopotential model is used to describe atomic binding of the alkali metals, and the two parameters are determined from experimental data (the model employs the Heine-Abarenkov potential with the Taylor dielectric function). (3) For each alkali metal (Li, Na, K, Rb, and Cs), the model is used to compute the pressure-versus-volume behavior and, at zero pressure, the binding energy, the density, and the elastic moduli and their pressure derivatives; the theoretical behavior is found to be in excellent agreement with experiment. (4) Calculations are made of κ, μ, and μ' of the bcc alkali metals over wide ranges of hydrostatic compression and expansion. (5) The pseudopotential results are compared with those of arbitrary—central-force models (wherein $\kappa-\frac{2}{3}\mu=\mu'+2P$) and with the specific Morse-function results. The pressures, bulk moduli, and zero-pressure shear moduli (as determined for the Morse and pseudopotential models) are in excellent agreement, but important differences appear in the shear moduli under high compressions. The computations in the present paper are for the bcc metals; a subsequent paper will extend this work to include both the bcc and fcc structures, at compressions and expansions where elastic stability or lattice cohesion is, in practice, lost.

I. INTRODUCTION

This is the first of two papers in which a pseudopotential model for atomic binding is used to study the theoretical behavior of the alkali metals under hydrostatic pressure. In this paper, we compute pressure derivatives of the elastic moduli at zero pressure as well as well as the pressure dependencies of the binding energies, the volumes, the bulk moduli, κ, and the shear moduli μ and μ'.[1-4] We use a two-parameter pseudopotential that employs the Heine-Abarenkov local model potential[5] and the Taylor approximation[6] for electron correlation and exchange. The numerical values of the two model parameters are determined for each metal (Li, Na, K, Rb, Cs) by (i) matching the theoretical and experimental lattice parameters and (ii) obtaining a best least-squares fit between the theoretical and experimental values of the three zero-pressure elastic moduli (atmospheric and zero pressure are taken as synonomous here).

Important considerations in our decision to carry out this study and in our selection of the pseudopotential model as a basis for computation are as follows.

(1) In recent years, advances have been made in the methodology for studying the theoretical elastic response of cubic crystals to hydrostatic pressure, including the use of (i) more physically meaningful definitions of the elastic moduli and (ii) rigorous conditions for the assessment of elastic stability under current loading conditions.[1-4] Earlier computations[1-3] of the variations with pressure of κ, μ, and μ', based upon Morse functions,[7] have provided useful insights into crystal elasticity and stability; they also raised a number of questions, e.g., "which of the results were essentially model dependent and which were dependent mainly upon crystal geometry or symmetry?" Another question is "how would the results (for the crystals with the central force interatomic interactions) compare with those of crystals with more realistic descriptions of atomic binding?" Although a variety of semiempirical models[8-11] are available, we selected the pseudopotential model for our elastic moduli,[1,2] and stability[3,12] studies for reasons indicated below.

(2) Various pseudopotential models are known to provide good descriptions of bonding in the alkali metals; specific studies have included evaluations of binding energies, elastic constants, and phonon dispersion curves,[13-17] the Gruneisen parameters and related properties,[13,18] higher-order elastic constants,[18,19] and comparisons of different crystal structures[20-22] (the references listed are representative rather than exhaustive). Studies involving deformation of the alkali metals include computations of the energy barrier for a bcc-fcc transition in Na (Ref. 23) and the variation of the volume and Green's elastic moduli with pressure in the range of 0—10 kbar (Ref. 24); the latter study neglected band-structure contributions to the binding energy (which are included in the present computations). Among various pseudopotential models, use of the Heine-Abarenkov and the Ashcroft[25] potentials has been popular; Sen and Sarker[13] carried out a "unified approach" pseudopotential study and concluded that the Heine-Abarenkov potential gave better results than the

Ashcroft for the alkalis. In particular, they showed that the two parameter Heine-Abarenkov model potential used with Taylor's dielectric function (i.e., the model for atomic binding used in the present work) gave very good results for calculated properties of the unstressed alkali metals.

(3) For the bcc alkali metals, experimental data are available for the elastic moduli and their pressure derivatives at atmospheric pressure and for the pressure versus volume relations (generated by both static and shock techniques) over wide pressure ranges. Thus, a variety of comparisons can be made between theory and experiment. In addition, the heavier bcc metals undergo phase transformations at high pressures and the lighter bcc metals transform at low temperature. This enables correlations to be made between our theoretical phase stability computations and the observed transformations [and, as is discussed in a subsequent paper, the theoretical results can (and do) provide insight into the nature and cause of the transformations]. Finally (in view of difficulties associated with high pressure measurements) the computations can (and indeed do) exhibit interesting behaviors not yet observed experimentally.

II. THEORY

A. Elastic moduli

The three elastic moduli κ, μ, and μ' for a cubic crystal in a current state of hydrostatic loading are defined[2] according to

$$\begin{aligned}&\dot\sigma_{11}+\dot\sigma_{22}+\dot\sigma_{33}=3\kappa(\epsilon_{11}+\epsilon_{22}+\epsilon_{33})\,,\\&\dot\sigma_{11}-\dot\sigma_{22}=2\mu(\epsilon_{11}-\epsilon_{22})\,,\\&\dot\sigma_{12}=2\mu'\epsilon_{12}\,,\end{aligned}\tag{1}$$

where the Cauchy stress is σ_{ij}, the Eulerian strain rate is ϵ_{ij}, and the overdot above the σ_{ij} denotes derivatives of components on cubic axes (or indeed on any rotating frame, when the current stress $\sigma_{ij}=-P\delta_{ij}$). Thus, κ is the bulk modulus and μ and μ' are the shear moduli in the relation between the cubic-axes components of the Cauchy stress increment and the rotationless strain increment (evaluated relative to the current configuration under pressure P). Stability of the crystal at any stage of hydrostatic loading is assessed according to[3,4,12]

$$\kappa(P)>0,\quad \mu(P)>0,\quad \text{and } \mu'(P)>0\,.\tag{2}$$

The present work emphasizes the moduli κ, μ, and μ', although various other moduli have been employed in the literature. In pioneering work, Born and his associates[26–28] studied crystal elasticity at finite strain from the "viewpoint" of the Green moduli; this latter viewpoint had since been popularly adopted in the literature. More generally, elastic moduli can be defined according to

$$C_{rs}\equiv\frac{1}{\Omega_0}\frac{\partial^2 E_{\text{bind}}}{\partial q_r\partial q_s}\,,$$

where E_{bind} is the binding energy per atom, Ω_0 is the reference volume per atom, and the q_r are generalized coordinates used to specify strain. Hill and Milstein[3,4] derived general relationships between sets of moduli C_{rs} and κ, μ, and μ'. If the coordinates q_r are taken as the independent components of some general tensor measure of strain and $e(\lambda)$ is a monotonic "scale function" with $e(1)=0$, $e'(1)=1$ [normalizations that ensure coincidence with the classical infinitesimal strain when the deformation is first order (see Refs. 29 and 30)] for cubic symmetry,

$$\begin{aligned}&\frac{(e')^2}{\lambda}C_{11}=\kappa+\tfrac{4}{3}\mu+\frac{\lambda e''}{e}P\,,\\&\frac{(e')^2}{\lambda}C_{12}=\kappa-\tfrac{2}{3}\mu-P\,,\\&\frac{(e')^2}{\lambda}C_{44}=\mu'+\tfrac{1}{2}P\left[1+\frac{\lambda e''}{e'}\right],\end{aligned}\tag{3a}$$

where λ is the all-round stretch; the stretch λ of any fiber is defined as its current length divided by its initial or reference length. Simple examples of the scale function are $\frac{1}{2}(\lambda^2-1)$, $(\lambda-1)$, or $\ln\lambda$. The first of these generates the relations between the Green moduli C_{rs} (wherein the q_r are specifically the Green strain variables) and κ, μ, and μ', viz.,

$$\begin{aligned}&C_{11}=(\kappa+\tfrac{4}{3}\mu+P)/\lambda\,,\\&C_{12}=(\kappa-\tfrac{2}{3}\mu-P)/\lambda\,,\\&C_{44}=(\mu'+P)/\lambda\,.\end{aligned}\tag{3b}$$

The second yields the relationships between the stretch moduli C_{rs} (introduced into lattice mechanics by Macmillan and Kelly[31]) and κ, μ, and μ', viz.,

$$\begin{aligned}&C_{11}=(\kappa+\tfrac{4}{3}\mu)\lambda\,,\\&C_{12}=(\kappa-\tfrac{2}{3}\mu-P)\lambda\,,\\&C_{44}=\left[\mu'+\frac{P}{2}\right]\lambda\,.\end{aligned}\tag{3c}$$

For the purpose of deriving computational formulas (and performing computations of moduli using atomic models), the nontensorial set of q_r, consisting of the edges of the deformed crystal cell and their included angles, is a particularly convenient choice; for this case[3,4]

$$\begin{aligned}&C_{11}=(\kappa+\tfrac{4}{3}\mu)\lambda\,,\\&C_{12}=(\kappa-\tfrac{2}{3}\mu-P)\lambda\,,\\&C_{44}=(\mu'+P)\lambda^3\,.\end{aligned}\tag{3d}$$

At *zero pressure*, Eqs. (3) of course all yield the "familiar" results $\mu'=C_{44}$, $\mu=\frac{1}{2}(C_{11}-C_{12})$, and $\kappa=\frac{1}{3}(C_{11}+2C_{12})$, and the stability criteria [conditions (2)] become equivalent to (what is commonly referred to as) the Born "stability criteria" (i.e., $C_{11}+2C_{12}>0$, $C_{11}-C_{12}>0$, and $C_{44}>0$). Although various investigators have invoked the Born criteria in the assessment of elastic stability of crystals under load, Milstein and Hill[3,12] have termed these criteria as "notional" and have shown them to be inadequate for the assessment of stabili-

ty of cubic crystals under hydrostatic pressure. In particular, the Born criteria are thoroughly relative (i.e., dependent upon choice of strain variable q_r in the definition of the C_{rs}) and the application of these criteria yields large quantitative and qualitative divergences from the stability ranges determined by the rigorous criteria [given by the conditions (2)].

Wallace[32] employed "stress-strain coefficients" B_{rs} which are closely related to the moduli of present interest, and gave relations [Ref. 32, p. 37, Eq. (3.38)] which are essentially equivalent to Eq. (3b). Wallace also presents calculations of B_{rs} and their first derivatives with respect to pressure (at zero pressure; i.e., $\lambda=1$) for a pseudopotential model of aluminum. The emphasis in the present paper is the domain of nonzero pressure, where the computational formulas are more complex and the physical phenomena (particularly regarding elastic stability and phase transitions) are more varied.

In Refs. 1 and 2, Milstein and Hill derived expressions for calculating (as functions of all-round stretch λ) the pressure $P(\lambda)$, the bulk modulus $\kappa(\lambda)$, and the shear moduli $\mu(\lambda)$ and $\mu'(\lambda)$ for cubic Bravais crystals in which the atomic bonds are modeled by pairwise interaction energies ϕ depending only on current separation between the atoms, viz.,

$$\begin{aligned} P(\lambda)&=-\frac{1}{3\Omega_0\lambda}\sum\delta^2\phi'(r^2)\ , \\ \kappa(\lambda)&=\frac{1}{9\Omega_0\lambda}\left[2\lambda^2\sum\delta^4\phi''(r^2)-\sum\delta^2\phi'(r^2)\right]\ , \\ \mu(\lambda)&=\frac{\lambda}{\Omega_0}\sum[(\delta_1^4-\delta_1^2\delta_2^2)\phi''(r^2)]-P(\lambda)\ , \\ \mu'(\lambda)&=\frac{2\lambda}{\Omega_0}\sum[\delta_1^2\delta_2^2\phi''(r^2)]-P(\lambda)\ , \end{aligned} \tag{4}$$

where the summations are over pairwise interactions, $\phi'(r^2)$ and $\phi''(r^2)$ are, respectively, the first and second derivatives of ϕ with respect to r^2 (the square of the magnitude of the lattice vector $\mathbf{r}$ connecting two lattice sites in the crystal), and the δ_i are the components of $\mathbf{r}$ in the unstressed or reference state. The bulk modulus can also be expressed as

$$\kappa(\lambda)=\frac{2\lambda}{3\Omega_0}\sum[(\delta_1^4+2\delta_1^2\delta_2^2)\phi''(r^2)]+P(\lambda)\ . \tag{5}$$

Thus, in the central potential model,

$$\kappa-\tfrac{2}{3}\mu=\mu'+2P\ , \tag{6}$$

as given by Milstein and Hill [Ref. 2, Eq. (2.6)]; this can be considered as a generalization of the Cauchy condition $C_{12}=C_{44}$ for central forces, in the sense that, at $P=0$, $\kappa-\frac{2}{3}\mu=\mu'$ is equivalent to $C_{12}=C_{44}$.

Milstein and Hill used Eqs. (4) to compute the pressure and the bulk and shear moduli of the entire Morse-model family of fcc, bcc, and sc monatomic crystals under arbitrary volumetric deformation.[1-3] Apparently these were the first theoretical computations of the shear moduli of cubic crystals, over wide ranges of hydrostatic loading (based on any reasonable atomic model), to have appeared in the literature; the essential elastic behavior was characterized in terms of the roles of (i) a "potential range indicator," β (ii) the crystal structure, and (iii) the all-round stretch λ. In Refs. 3 and 12, Milstein and Hill used their bulk and shear moduli computations to determine the stable ranges (and potential bifurcations at the range limits) of the entire Morse-model family of fcc, bcc, and sc monatomic crystals under constant hydrostatic compression and tension. While the Morse-function description of crystals often yields realistic results (quantitatively), particularly for fcc crystals,[33-35] and the bulk and shear moduli computations have provided numerous insights into the nature of crystal elasticity and stability under pressure,[1-3,12] this description also suffers from several limitations. The most serious are that the model for atomic binding is empirical and lacks a fundamental basis in quantum theory, the crystal model exhibits "Cauchy symmetry" [i.e., the moduli obey Eq. (6)], whereas most real crystals do not, and, in general, the shear moduli of bcc crystals are poorly represented [e.g., at zero pressure, the ratio of shear moduli μ/μ' does not exceed about 0.2 for Morse-function bcc crystals,[2] whereas experimental values for bcc metals are in the range of about 0.1 (for the alkali metals) to 2.0 (for chromium)].

In view of these considerations, it is desirable to extend the Milstein and Hill computations of the pressure-dependent behavior of the moduli κ, μ, and μ' (and associated domains of stability) by employing more realistic, quantum-based models. Thus, in the present study, we use the pseudopotential model (described in the following section) to represent the binding energy E_{bind} in computations of the pressure P and the elastic moduli κ, μ, and μ' as functions of all-round stretch λ. The formulas used in these computations are derived in the Appendix. This paper deals exclusively with the bcc structures (since these are the structures for which experimental data on elastic properties are available); a subsequent paper extends the computations to include the fcc crystals, since these are also important in understanding phase stability.

B. Pseudopotential model

In pseudopotential theory,[5] a simple *sp*-bonded metal has a binding energy per atom represented by

$$E_{\text{bind}}=E_{\text{fe}}+E_{\text{es}}+E_{\text{bs}}\ . \tag{7}$$

The three terms are the free-electron energy, the electrostatic energy, and the band-structure energy, respectively. The free-electron energy can be written as

$$E_{\text{fe}}=z\left\{\alpha\left[\frac{z}{\Omega}\right]+5.742\left[\frac{z}{\Omega}\right]^{2/3}-1.477\left[\frac{z}{\Omega}\right]^{1/3}-0.031\ln\left[\left[\frac{z}{\Omega}\right]^{1/3}\right]-0.130\right\}\ , \tag{8}$$

where z is the valence (taken as unity for the alkali metals) and Ω is the atomic volume. (The units of energy and length are, respectively, Rydbergs and Bohr radii; $\hbar=2m_e=e^2/2=1$, where e is the charge on an electron and m_e is the electron mass.) The first term in Eq. (8) is the core correction of the pseudopotential, where α is a

constant dependent upon the choice of pseudopotential. The kinetic energy and exchange interactions of a free-electron gas are represented by the second and third terms, respectively, and the final two terms are corrections for electron correlation, as given by the Nozières-Pines formulation.

For a Bravais lattice, the electrostatic and band-structure energies are represented as

$$E_{es}+E_{bs}=-\frac{z^2\pi}{\eta\Omega}-\frac{2z^2\eta^{1/2}}{\pi^{1/2}}+\frac{2z^2}{\pi^{1/2}}\sum_{\mathbf{r}}{}'\frac{1}{r}\int_{\eta^{1/2}r}^{\infty}e^{-x^2}dx+\frac{4\pi z^2}{\Omega}\sum_{\mathbf{q}}{}'\frac{[e^{-q^2/4\eta}-F_n(q)]}{q^2}\,. \tag{9}$$

The first summation is over real lattice vectors $\mathbf{r}$ and the second summation is over reciprocal-lattice vectors $\mathbf{q}$. (The primes on the sums imply that the origins are omitted.) Equation (9) has the mathematical property that the numerical value of $E_{es}+E_{bs}$ is independent of the value of the parameter η (Ref. 5, p. 365). However, the rate of convergence of each of the summations does depend on η; thus it is desirable to choose η so that the computational time needed to evaluate $E_{es}+E_{bs}$ is kept relatively low. In the present computations, this was accomplished by choosing a value of η that caused the summations of each term [$e^{-q^2/4\eta}$ and $F_n(q)$] in the reciprocal-lattice summation to converge at approximately the same value of q (specifically, η was approximately 0.05). The quantity $F_n(q)$ is the normalized wave-number characteristic, which can be written as

$$F_n(q)=\frac{\Omega^2q^2}{8\pi z^2}V^2(q)\frac{\Pi(q)}{\epsilon(q)}\,, \tag{10}$$

where $V(q)$ is the Fourier transform of the selected model potential and $\epsilon(q)$ is the electron-gas dielectric function. [$F_n(q)$ is related to the more usual energy wave-number characteristic $F(q)$ by $F_n(q)=-(q^2\Omega/4\pi z^2)F(q)$.] For the electron-gas dielectric function[6]

$$\epsilon(q)=1+\frac{8\pi}{q^2}\Pi(q)\,, \tag{11}$$

where

$$\Pi(q)=\frac{\chi(q)}{1-\frac{8\pi}{q^2}f(q)\chi(q)} \tag{12}$$

with

$$\chi(q)=\frac{k_f}{4\pi^2}\left[1+\frac{1-\eta_f^2}{2\eta_f}\ln\left|\frac{1+\eta_f}{1-\eta_f}\right|\right]. \tag{13}$$

The variable $\eta_f=q/2k_f$, and the Fermi wave number $k_f=(3\pi^2z/\Omega)^{1/3}$. The quantity $f(q)$ in Eq. (12) is included to account for electron correlation and exchange; following Taylor,[6] $f(q)$ is taken as

$$f(q)=\eta_f^2\left[1+\frac{0.1534}{\pi k_f}\right]. \tag{14}$$

The Heine-Abarenkov model potential Fourier transformed is given by[14]

$$V(q)=-\frac{8\pi z}{\Omega q^2}\left[(1+u)\cos(qR_m)-u\frac{\sin(qR_m)}{qR_m}\right], \tag{15}$$

where R_m and u are model matching parameters. The parameter R_m represents the ionic radius and $2zu/R_m$ represents the depth of the potential well within the ionic radius. The constant α in E_{fe} for this pseudopotential is given by

$$\alpha=\frac{4\pi}{3}R_m^2(2u+3)\,. \tag{16}$$

Following usual practice (Ref. 5, p. 302), Eq. (15) was multiplied by the damping factor $\exp(-0.03\eta_f^4)$ in the computations to dampen nonphysical oscillations in the pseudopotential. (The addition of the damping factor improves the convergence of the reciprocal space sum considerably, but affects the elastic constants by at most a few percent.)

The numerical values of R_m and u can be determined by obtaining "best fits" of theoretically computed properties to the corresponding experimental properties. For the present study, it was considered important that the density and elastic properties of the theoretical models of each metal be in good agreement with the corresponding experimental values. Thus, the model parameters R_m and u were determined by matching the experimental lattice constant and obtaining a best least-squares fit to the three zero-pressure elastic moduli (i.e., R_m and u were "adjusted" so that the theoretically computed pressure is zero when Ω is equal to the experimental value of Ω_0 and that the best least-squares fit is obtained between the experimental and the theoretically computed elastic moduli κ, μ, and μ' at $P=0$). (Computational details are provided in the Appendix.) Table I lists the values of u and R_m determined in this manner, as well as the experimental and theoretical values of the zero-pressure lattice parameters a_0 and elastic moduli for the five alkali metals. It is noted that the *two-parameter*-model formulation yields excellent agreement between the experimental and theoretical values of the *four quantities* a_0, κ, μ, and μ' (at $P=0$). Additional comparisons between theoretical and experimental results are presented in Sec. III.

III. THEORETICAL RESULTS

In this section, we present the results of using the pseudopotential model, described in the preceding section (with the computational formulas derived in the Appendix), to compute the binding energies, pressures, and elastic moduli κ, μ, and μ' of the alkali metals over wide ranges of compression and expansion. Computed values of the binding energies and pressure derivatives of the moduli of the bcc metals at zero pressure are listed and compared with experimental values in Table II. Although the experimental values for the derivatives of the elastic moduli are based upon "room-temperature" data, while the computations are for 0 K, the respective theoretical and experimental values in Table II are remarkably close. (It is to be emphasized that none of the quantities listed in

TABLE I. Pseudopotential model parameters u and R_m and computed (theor) and experimental (expt) values of the zero-pressure lattice parameter a_0 and zero-pressure elastic moduli κ, μ, and μ' for the alkali metals; the experimental values are extrapolated to 0 K (Ref. 40). The considered crystal structure is bcc.

Metal	u	R_m (Bohr radii)	a_0	κ (kbars)	μ (kbars)	μ' (kbars)
Li (theor)	−0.291 24	1.511 62	6.5621	135.2	11.7	119.5
Li (expt)			6.5621	141.0	12.0	117.0
Na (theor)	−0.484 09	2.175 77	7.9403	75.2	7.38	64.2
Na (expt)			7.9403	76.7	7.0	63.0
K (theor)	−0.629 05	3.108 60	9.8624	37.2	3.95	29.4
K (expt)			9.8624	37.7	4.0	29.0
Rb (theor)	−0.627 95	3.387 00	10.5388	30.2	3.34	23.4
Rb (expt)			10.5388	31.7	2.5	22.0
Cs (theor)	−0.738 46	3.954 06	11.4205	22.4	2.47	16.6
Cs (expt)			11.4205	23.2	2.1	16.1

Table II were used in determining the empirical model parameters; thus, although the empirical parameters were determined from "harmonic behavior," the model provides a good description of anharmonic behavior.) In fact, given the difficulties associated with determining higher-order elastic moduli experimentally, it is our contention that the experimentally based values of the derivatives of the moduli are not to be considered superior to the computed values.

Additional evidence for the validity of the model is provided by Figs. 1(a) and 1(b) which show experimental and theoretical pressure-volume relations for the five alkali metals in their bcc configurations; the experimental results include static compression and shock-wave compression measurements.[36] (The plots are of pressure versus all-round stretch λ; to obtain the pressure-volume relations, the atomic volume Ω is readily computed from the stretch, i.e., $\Omega=\lambda^3\Omega_0$.) The agreement in Figs. 1(a) and

TABLE II. Theoretical (theor) and experimental (expt) binding energies and derivatives of the elastic moduli (at zero pressure) for the bcc alkali metals. The theoretical values are those computed in the present study using the pseudopotential model parameters listed in Table I, and the experimental values are based upon data found in the respective references; all experimental values were determined at or near room temperature.

Metal	E_{bind} (Ry)	$d\kappa/dP$	$d\mu/dP$	$d\mu'/dP$	$d^2\kappa/dP^2$ (kbars^{-1})	$d^2\mu/dP^2$ (kbars^{-1})	$d^2\kappa/dP^2$ (kbars^{-1})
Li (theor)	−0.574	3.58	0.268	1.74	−0.022	−0.0041	−0.029
Li (expt)	−0.517[a]	3.33[b]	0.100[c]	1.35[c]			
Li (expt)		3.62[b]					
Na (theor)	−0.466	3.71	0.264	1.53	−0.045	−0.0081	−0.054
Na (expt)	−0.460[a]	3.83[d]	0.258[d]	1.45[d]	−0.019[e]		
Na (expt)		3.68[b]			−0.37[e]		
Na (expt)		3.97[b]					
K (theor)	−0.389	3.76	0.268	1.25	−0.10	−0.018	−0.11
K (expt)	−0.388[a]	3.97[f]	0.251[f]	1.62[f]	−0.039[e]		
K (expt)		3.63[b]			−0.052[e]		
K (expt)		3.75[b]					
Rb (theor)	−0.368	3.77	0.268	1.16	−0.13	−0.023	−0.13
Rb (expt)	−0.370[a]	3.65[g]	0.229[g]	1.48[g]	−0.009[e]		
Rb (expt)		3.39[b]			−0.026[e]		
Rb (expt)		3.93[b]					
Cs (theor)	−0.344	3.72	0.271	1.07	−0.19	−0.033	−0.17
Cs (expt)	−0.345[a]						

[a]C. Kittel, *Introduction to Solid State Physics*, 5th ed. (Wiley, New York, 1976).
[b]R. Groover, J. Phys. Chem. Solids **32**, 2539 (1971).
[c]A. L. Jain, Phys. Rev. **123**, 1234 (1961).
[d]R. H. Martinson, Phys. Rev. **178**, 902 (1969).
[e]S. N. Vaidya, I. C. Getting, and G. C. Kennedy, J. Phys. Chem. Solids **32**, 2545 (1971).
[f]P. A. Smith and C. S. Smith, J. Phys. Chem. Solids **26**, 279 (1965).
[g]D. Sen and S. K. Sarkar, Phys. Rev. B **22**, 1856 (1979).

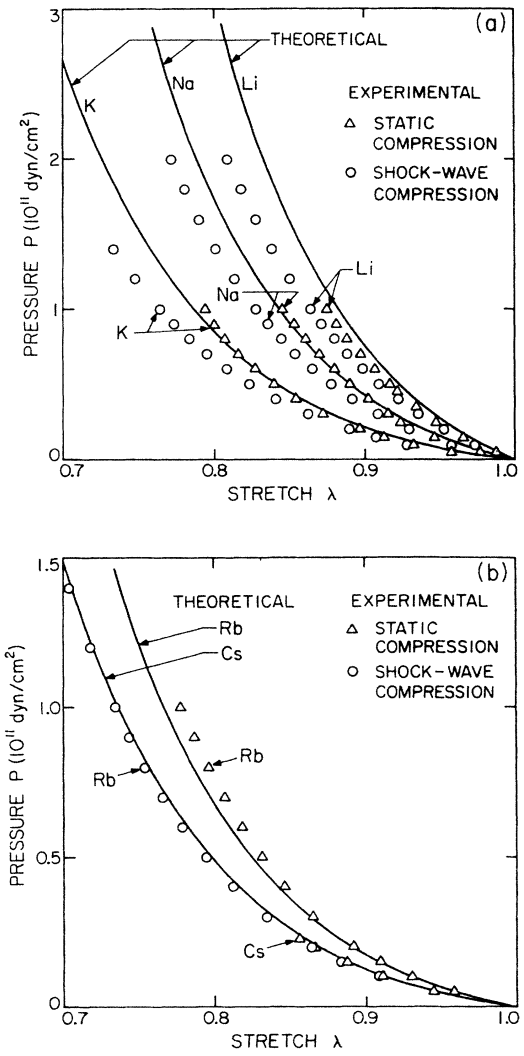

FIG. 1. Comparison of theoretical and experimental pressure-volume relations: (a) lithium, sodium, and potassium; (b) rubidium and cesium.

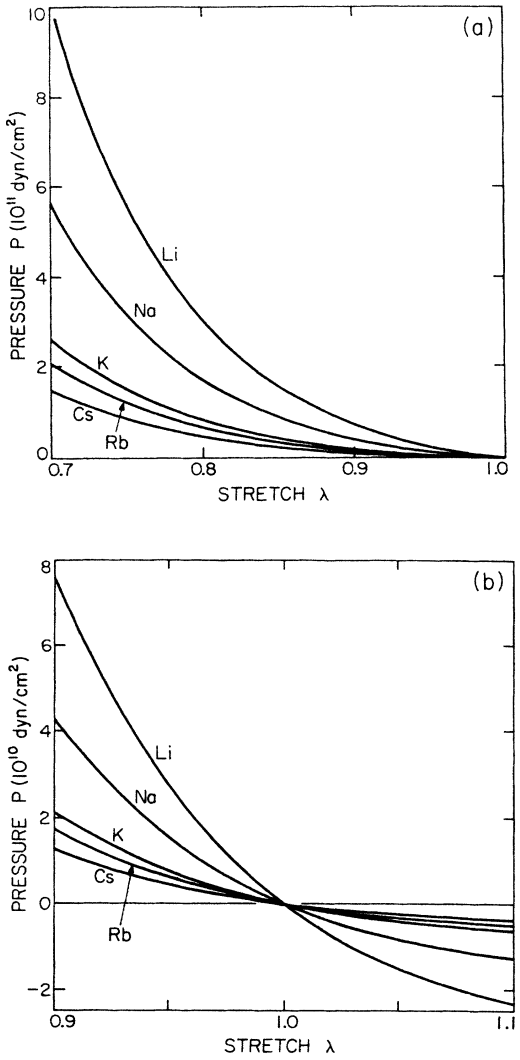

FIG. 2. Pressures versus stretch for the bcc alkali metals: (a) compression; (b) compression and expansion in the neighborhood of the zero-pressure states.

1(b) between theory and experiment is excellent, particularly for the "static compression" data, which, for all of the metals, are very close to the theoretical results. This agreement therefore provides further justification for use of the pseudopotential model in computing the elastic moduli of the alkali metals over wide pressure ranges. In particular, it is a basic assumption in pseudopotential theory for simple *sp*-bonded metals that the core states are localized and small.[37]. This small core approximation implies that the cores interact only by Coulombic repulsion, and that the core states are relatively unaffected by interatomic phenomena (e.g., by the crystal structure or variations in interatomic spacing caused by changes in the loading environment). The effective isolation of the core states leads to the static core approximation used here, that is, u and R_m are taken to be constant. In view of the agreement between experiment and theory found in Tables I and II and Figs. 1(a) and 1(b) this assumption appears to be justified at very high compressions, as well as at zero pressure. [It might be noted that the experimental data shown in Figs. 1(a) and 1(b) are for room temperature, whereas the theoretical results correspond to 0 K. However, static measurements for lithium, sodium, and potassium, made over a pressure range of about 0—20 kbars at liquid-helium temperatures,[38] show the change in the experimental data (in passing from room temperature to 0 K) to be considerably less than the difference between the static and shock data shown in Figs. 1(a) and 1(b)].

Investigators of pressure-dependent phenomena often use various empirical or semiempirical formulas to represent their results analytically. Although we have not attempted to fit our results to such formulas, we present some results in tabular form (see Table III) for the benefit of investigators who might be interested in such endeavors and to provide greater numerical accuracy than can be obtained from graphs; we also present the results graphically for ease of comparison among the various moduli and metals. The graphs (Figs. 2—5) follow the format that

TABLE III. Dependence of binding energy E_{bind}, pressure P, and elastic moduli κ, μ, and μ' upon stretch λ for the bcc alkali metals, as computed in the present work from the pseudopotential formulation described in Sec. II.

Metal	λ	$-E_{bind}$ (Ry)	P (kbars)	κ (kbars)	μ (kbars)	μ' (kbars)
Li	0.70	0.411 029	1 010.75	2 777.96	90.9813	537.294
	0.75	0.468 509	559.298	1 668.96	68.6026	445.594
	0.80	0.504 654	304.573	1 011.53	50.7657	354.550
	0.85	0.526 612	159.155	616.535	36.8883	275.534
	0.90	0.539 058	75.5375	375.985	26.1768	210.937
	0.95	0.545 084	27.4277	227.655	17.9593	159.654
	1.00	0.546 754	0.000 00	135.228	11.6976	119.543
	1.05	0.545 463	−15.2536	77.1821	6.961 89	88.4079
	1.10	0.542 165	−23.2948	40.5684	3.409 38	64.3344
Na	0.70	0.330 409	565.265	1510.52	41.8246	182.973
	0.75	0.387 719	316.592	931.851	35.5475	178.126
	0.80	0.424 066	173.230	573.717	27.7051	157.573
	0.85	0.446 193	90.4544	351.921	20.7598	131.590
	0.90	0.458 703	42.7284	214.296	15.1585	105.979
	0.95	0.464 723	15.3980	128.650	10.7743	83.2692
	1.00	0.466 379	0.000 00	75.1994	7.377 79	64.1916
	1.05	0.465 117	−8.391 04	41.7923	4.760 17	48.6367
	1.10	0.461 923	−12.6653	20.9394	2.752 84	36.1710
K	0.70	0.264 206	263.504	671.356	10.2548	49.2477
	0.75	0.315 999	151.188	428.944	13.3558	55.5129
	0.80	0.349 555	84.2322	272.301	12.4042	55.9580
	0.85	0.370 293	44.5045	170.911	10.1112	51.5015
	0.90	0.382 125	21.1552	105.611	7.71583	44.4947
	0.95	0.387 843	7.637 04	63.8164	5.637 75	36.7799
	1.00	0.389 417	0.000 00	37.2285	3.954 27	29.4218
	1.05	0.388 222	−4.134 88	20.4258	2.628 34	22.9076
	1.10	0.385 217	−6.198 77	9.987 14	1.597 21	17.3827
Rb	0.70	0.245 036	210.106	528.139	5.446 26	29.3875
	0.75	0.295 590	121.368	340.650	9.473 35	36.7547
	0.80	0.328 544	67.9751	218.147	9.564 99	39.7704
	0.85	0.349 001	36.0435	137.855	8.108 59	38.3033
	0.90	0.360 705	17.1676	85.571 6	6.328 15	34.1106
	0.95	0.366 369	6.201 58	51.819 2	4.696 58	28.8019
	1.00	0.367 928	0.000 00	30.217 0	3.340 53	23.4030
	1.05	0.366 746	−3.351 48	16.514 1	2.257 42	18.4431
	1.10	0.363 777	−5.013 64	7.914 40	1.407 42	14.1345
Cs	0.70	0.232 251	148.596	369.039	2.052 35	26.0724
	0.75	0.277 914	86.54 30	238.855	5.468 30	26.6352
	0.80	0.307 951	48.84 07	154.546	6.286 85	27.3718
	0.85	0.326 774	26.18 98	98.8951	5.695 00	26.3011
	0.90	0.337 636	12.57 20	62.1378	4.600 33	23.6653
	0.95	0.342 929	4.569 48	38.0279	3.465 35	20.2119
	1.00	0.344 393	0.000 00	22.3653	2.468 14	16.5696
	1.05	0.343 278	−2.488 16	12.3012	1.650 73	13.1252
	1.10	0.340 470	−3.728 65	5.917 61	1.002 22	10.0664

each (a) figure presents the results for all five alkali metals over a large range of compressive stretch while each (b) figure "enlarges" the results in the neighborhood of the zero-pressure ($\lambda=1$) state [the ordinate scales of the respective (a) and (b) figures differ by about an order of magnitude]. The (b) figures also include a range of hydrostatic expansion ($\lambda>1$). As noted by Milstein and Hill,[3] "states of pure hydrostatic tension can be approach locally near cracks and other stress raisers. Since controlled experimentation with this type of loading is fraught with difficulties, a special significance is attached to the theoretical moduli."

A variety of interesting behaviors are observed in Table III and Figs. 2–5. At $\lambda=1$, of course, the pressures are

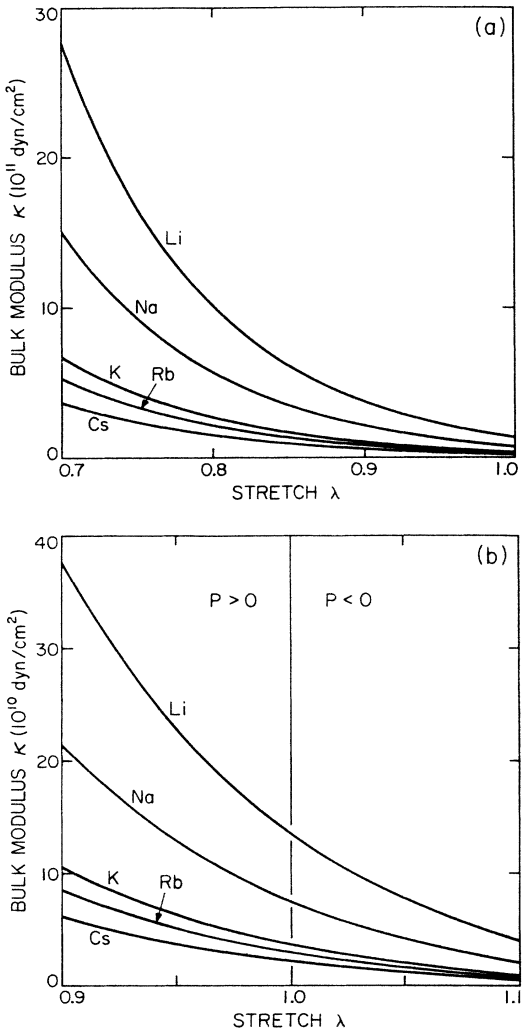

FIG. 3. Bulk moduli versus stretch for the bcc alkali metals: (a) region of compression; (b) spanning regions of compression and expansion near the zero-pressure states.

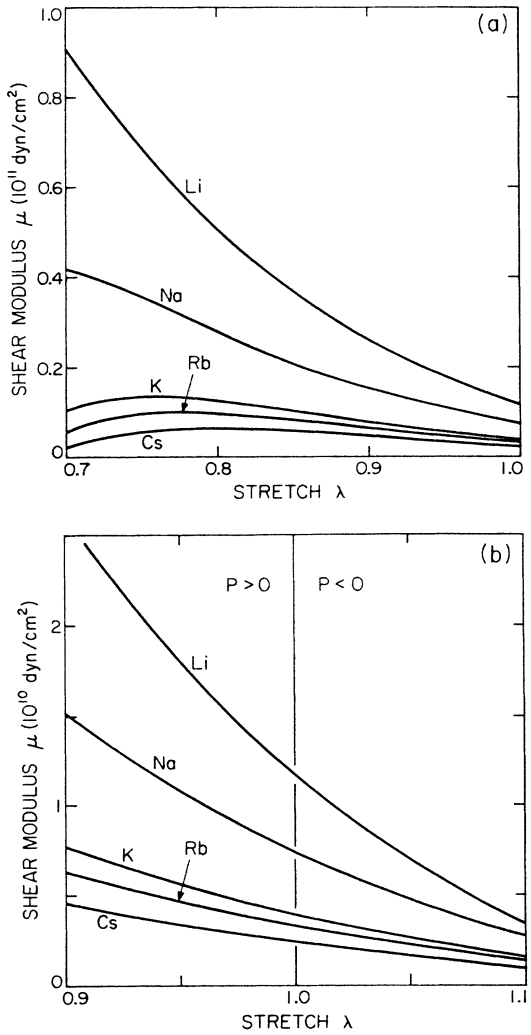

FIG. 4. Shear moduli μ versus stretch for the bcc alkali metals: (a) region of compression; (b) spanning regions of compression and expansion near the zero-pressure states.

all zero, the binding energies are at their minima, and the lattice parameter of each metal is equal to its respective experimental value at zero pressure and temperature [as λ departs from unity, the binding energy must increase, while the pressure must either increase (if $\lambda<1$) or decrease (if $\lambda>1$)]. For a given value of λ, within the range of these figures, the magnitudes of the pressures and of each of the moduli are ordered according to $\chi_{\mathrm{Li}}\geq\chi_{\mathrm{Na}}\geq\chi_{\mathrm{K}}\geq\chi_{\mathrm{Rb}}\geq\chi_{\mathrm{Cs}}$, where χ_M represents the particular modulus (κ, μ or μ') or the pressure of the element indicated by the subscript M; thus, among the alkali metals, the smaller the "ionic radius" R_m (and zero-pressure lattice parameter a_0), the "stiffer" the metal (i.e., the greater its resistance to compressive as well as shearing stresses), not only in the reference state, but over wide ranges of compression and expansion. Also, for each metal, the shear moduli are ordered according to $\mu'(\lambda)>\mu(\lambda)$ (at a given value of λ). Thus, shearing is easier relative to the $\langle 110\rangle$ axes of the bcc metals than to the $\langle 100\rangle$ axes, not only at zero pressure, but over wide ranges of hydrostatic compression and expansion. In compression, the pressures and bulk moduli increase monotonically with decreasing stretch; initially (i.e., in the neighborhood of $\lambda=1$), the shear moduli also increase with decreasing stretch, but deviations from monotonic behavior are found at large compressions. In particular, the shear moduli $\mu(\lambda)$ and $\mu'(\lambda)$ of the bcc metals pass through maxima which are found at successively lower values of stretch and higher pressures as the atomic number of the metal decreases (i.e., in passing through the series from Cs to Li). At still greater compressions [not shown in Figs. 4(a) or 5(a)], the functions $\mu'(\lambda)$ pass through positive minima and the functions $\mu(\lambda)$ pass through negative minima; both functions then increase rapidly with further decreases in λ. Thus, each modulus $\mu(\lambda)$ passes through a zero (which terminates a stable region for the respective bcc metal); this is discussed in detail in a subsequent paper. For each metal in compression, and over an initial range of expansion, the bulk modulus is greater than the shear moduli (at a given pressure or stretch), but at larger values of λ (in hydrostatic expansion), $\kappa(\lambda)$ successively drops below $\mu'(\lambda)$ and $\mu(\lambda)$. In expansion, for each bcc

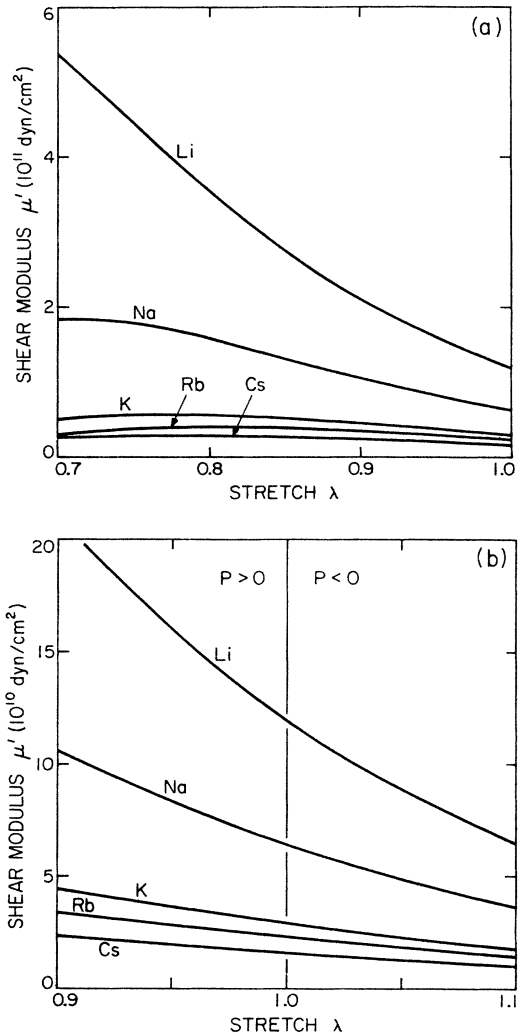

FIG. 5. Shear moduli μ' versus stretch for the bcc alkali metals: (a) region of compression; (b) spanning regions of compression and expansion near the zero-pressure states.

metal except Li, the onset of elastic instability is found to be coincident with $\kappa(\lambda)=0$, as is also discussed in detail in a subsequent paper.

It should be emphasized that each of the present pressure and moduli computations was carried out (using the pseudopotential model described in the preceding section and the expressions in the Appendix) for the lattice in a *current* state of compression or expansion, rather than from series expansions based on higher-order moduli computed for the reference ($\lambda=1$) state. In this connection, it is noted that all of the "modulus versus λ" plots exhibit significant departures from linearity. Thus, the results shown graphically in Figs. 2–5 could not have been closely approximated by use of series expansions based on the higher-order elastic moduli C_{ijk} evaluated in the reference state; in fact, given the various shear moduli maxima, expansions including even the fourth-order moduli in the reference state,

$$C_{ijkl}=(\partial^4 E_{\text{bind}}/\partial q_i \partial q_j \partial q_k \partial q_l)_{\lambda=1} ,$$

would provide grossly inadequate descriptions of the $\mu(\lambda)$ and $\mu'(\lambda)$ functions in Figs. 4(a) and 5(a).

A classical problem in crystal elasticity is: "to what extent can elastic properties be represented accurately by central-force models of interatomic interactions?" This is also a problem of practical importance since central-force models are the simplest to deal with mathematically and computationally. Quantitative considerations of this problem are usually restricted to either the general elastic properties in the unstressed state of the crystal or to just the pressure-volume relationships. For example, it is well known that, in general, a central-force model can represent accurately only two of the three elastic moduli of an unstressed cubic crystal since the model yields $C_{12}=C_{44}$, whereas the moduli of most real cubic crystals exhibit departures from this relation; the degree of departure provides information about the relative importance of noncentral forces in the particular crystal. With the aid of Eq. (6) and our pseudopotential computations, we can extend such considerations to general elastic properties of the bcc alkali metals over a wide range of hydrostatic deformation. According to Eq. (6), only three of the four quantities κ, μ, μ', and P vary independently in any central-force model, and thus the general elastic properties of a cubic crystal under pressure can be accurately modeled by purely central forces between atoms only if the ratio $(\mu'+2/3\mu)/(\kappa-2P)$ for the crystal is close to unity. Deviations of this ratio from unity must be owing to noncentral-force contributions to the binding energy, which, in the present pseudopotential computations, arise from the volume-dependent electron-gas and electrostatic contributions. Within the range of compressive deformation represented in Figs. 1(a) and 1(b) and Figs. 2(a), 3(a), 4(a), and 5(a), this ratio tends to be closest to unity in the vicinity of the unstressed state ($\lambda=1$). For Li, throughout this range, the ratio $(\mu'+2/3\mu)/(\kappa-2P)$ remains relatively close to unity (i.e., within about 0.8–1.0), as is seen in Fig. 6(a); Na starts (near its maximum) at about 0.92 at $\lambda=1$, initially remains relatively flat, and then drops to below 0.6 at $\lambda=0.7$; K, Rb, and Cs all start above 0.8 at $\lambda=1$ and decrease monotonically to below 0.4 at $\lambda=0.7$. Thus, in general, the deviation between the pseudopotential elasticity computations and any purely central-force computations becomes greater at very large pressures, with the effect more pronounced for the heavier alkali metals. When viewed over a wider range [Fig. 6(b)], the function $(\mu'+2/3\mu)/(\kappa-2P)$ is seen to undergo various oscillations, which, in part, can be associated with the oscillations in the functions $\mu(\lambda)$ and $\mu'(\lambda)$, mentioned earlier.

A central-force model was used by Milstein and Hill[2,3] in the first atomistically based computations of shear moduli of crystals under hydrostatic loading. In particular, they considered all atoms in the crystal to interact via a Morse function,

$$\phi(r)=D(e^{-2\alpha(r-r_0)}-2e^{-\alpha(r-r_0)}) ,$$

where D, α, and r_0 are empirical parameters that can be determined from experimental data. Although three pa-

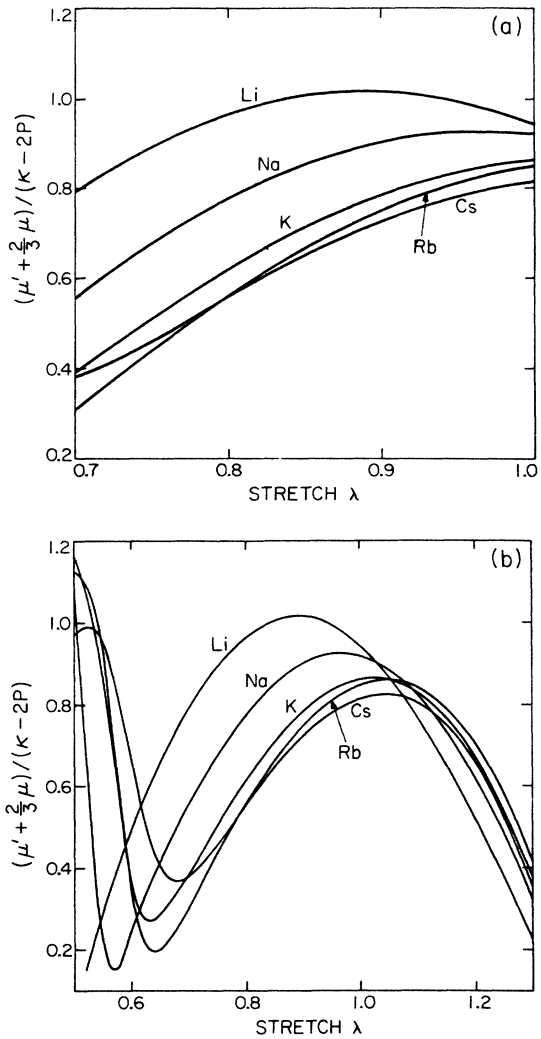

FIG. 6. Comparison of the elastic behavior of the bcc alkali metals (as described by the pseudopotential model) with that of any cubic crystal model consisting only of pairwise central-force interactions between atoms. For the "pairwise" model, the ratio represented on the ordinate scale would be unity throughout. (a) In compression, (b) over a large range of deformation, including compression and expansion.

rameters are needed to specify the Morse function, they showed analytically that, for a given crystal structure, the quantities $P(\lambda)/\kappa(1)$, $\kappa(\lambda)/\kappa(1)$, $\mu(\lambda)/\kappa(1)$, and $\mu'(\lambda)/\kappa(1)$ depend on only one such parameter, $\beta \equiv e^{ar_0}$. That is, for a given crystal structure and a given value of β, there is a unique function $P(\lambda)/\kappa(1)$ versus λ, likewise for $\kappa(\lambda)/\kappa(1)$ versus λ, and so on. [The same is true for the quantities $P(\lambda)/P(\lambda_0)$, $\kappa(\lambda)/\kappa(\lambda_0)$, $\mu(\lambda)/\mu(\lambda_0)$, and $\mu'(\lambda)/\mu'(\lambda_0)$, where λ_0 is any particular value of λ at which the pressure and the three moduli are nonzero.] They interpreted the Morse parameter β as a measure of the "effective range" of the potential ϕ, since larger values of β correspond to shorter range, steeper functions, and smaller values correspond to longer range and shallower functions. (As β becomes large, the behavior of the crystals approaches that of a collection of "hard spheres," with nearest-neighbor interactions only. Also, there exists a lower limit to the numerical value of β, for which the behavior of the crystal, in a sense, approaches that of a continuum.) The intermediate values of β (i.e., $\ln\beta = ar_0 \approx 3$ to 8) provide the most realistic models of actual crystals.

For the alkali metals, the Morse model with values of $\ln\beta$ in the neighborhood of 3 provides an excellent description of the $\kappa(\lambda)$ and $P(\lambda)$ behavior; this is seen in Fig. 7, which compares the pseudopotential and Morse-model computations of the pressures and bulk moduli ("normalized" by the respective zero-pressure bulk moduli). [In an earlier study (see Table III of Ref. 39), Milstein determined specific Morse-parameter values for potassium ($D = 0.11375 \times 10^{-12}$ erg, $a a_0 = 2.6061$, and $r_0/a_0 = 1.21963$, with $a_0 = 5.344$ Å), based upon the experimental values of the unstressed lattice parameter a_0 and the elastic constants C_{11} and C_{12}; thus for K, based on these values, $\ln\beta = 3.18$, in excellent agreement with the values of $\ln\beta$ that provide accurate descriptions of the pressure and bulk modulus versus stretch. Note that the three adjustable parameters in the Morse function can be adjusted independently so that the crystal has the correct (i.e., experimental) values of *unstressed* lattice parameter, bulk modulus, and shear modulus μ *or* μ'; the functions $\kappa(\lambda)/\kappa(1)$ or $\mu(\lambda)/\mu'(\lambda)$ then depend only upon the value of the one parameter $\ln\beta$.] Figure 7 also points out the interesting result that the "normalized" pressure curves are almost the same for all of the alkali metals (as are the bulk modulus curves), suggesting "almost" universal functions for $P(\lambda)/\kappa(1)$ and $\kappa(\lambda)/\kappa(1)$ among the alkalis; however, for the normalized shear moduli, no such "almost" universal curves [i.e., $\mu(\lambda)/\kappa(1)$ or $\mu'(\lambda)/\kappa(1)$] exist as is

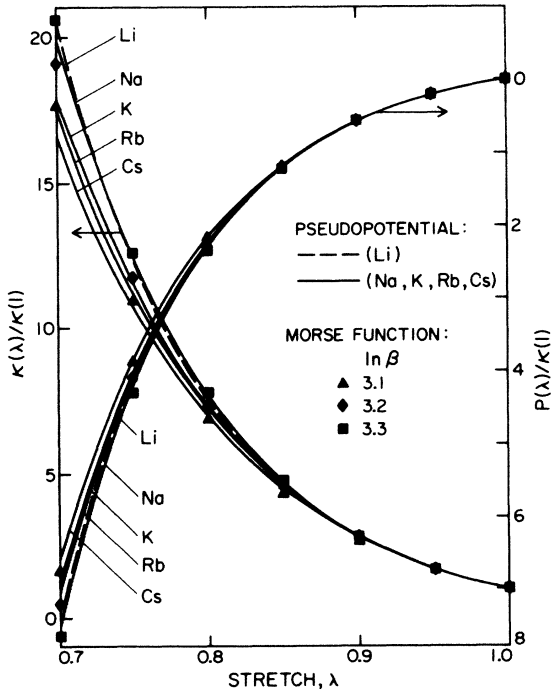

FIG. 7. Comparison of the Morse function (Ref. 1) and pseudopotential-model computations of the variations of the pressures and bulk moduli of the alkali metals in compression.

evident from Figs. 4(a) and 5(a).

Figure 8 shows that the Morse model, with $\ln\beta \approx 3$, also gives good representation to the shear moduli of the bcc alkalis near $\lambda = 1$, and predicts that the ratio μ/μ' initially increases with pressure, in qualitative agreement with the pseudopotential computations. However, despite this agreement and the Morse model's excellent representation of the pressure and bulk modulus in Fig. 7, divergences between the representations of the shear moduli in the Morse and pseudopotential models are inevitable [in view of Fig. 6(a)], particularly at higher pressures. These divergences are indeed evident in Fig. 8: while the ratio μ/μ' for the Morse-function crystals increases slowly and monotonically with increasing pressure, for the pseudopotential crystals it increases more rapidly with pressure initially, but then passes through a maximum and drops below the Morse-function values. Figure 8 shows that, in the range of compression $0.7 \leq \lambda \leq 1$, among the bcc alkalis, the shear moduli of Li are best approximated by the Morse model, in agreement with Fig. 6(a), which shows the general elastic behavior of Li to come closest to that of a crystal with purely central forces between atoms (irrespective of the particular model for the central forces).

The maxima observed in Fig. 8 are due to the "oscillations" in $\mu(\lambda)$ and $\mu'(\lambda)$, as discussed earlier. In the Morse-model computations, the functions $\mu(\lambda)$ for the complete family of bcc crystals had the same *qualitative* behavior as in the pseudopotential computations; i.e., there exists a positive local maximum, a zero, and a negative minimum. Thus the general behavior of $\mu(\lambda)$ appears to be a "structural phenomena" (i.e., not dependent upon the specific details of the pseudopotential or upon the presence of noncentral-force contributions to the binding energy), although the quantitative details are certainly model dependent. For example, in the Morse-function bcc crystals, the local maximum in $\mu(\lambda)$ was always in expansion ($\lambda > 1$), whereas in the present computations, it is always in compression; there are also important differences in the locations of the zeros of $\mu(\lambda)$, leading to differences in the predicted stable ranges; this is discussed at greater length in a subsequent paper. [See Ref, 2, p. 227, for a discussion of the roles of specific interatomic interactions in shaping the $\mu(\lambda)$ curves for bcc crystals.]

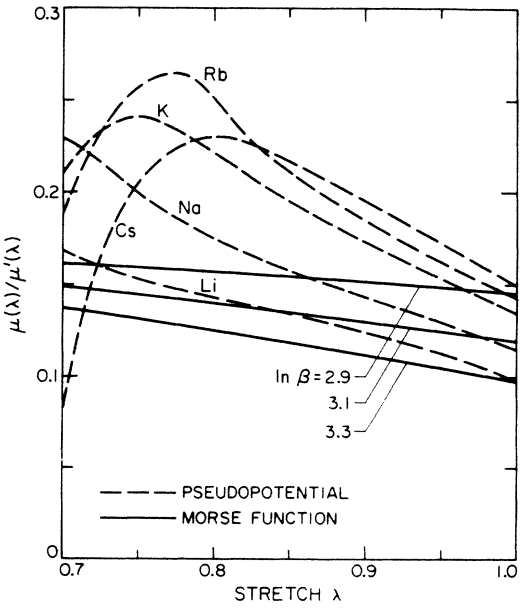

FIG. 8. Morse function (Ref. 2) and pseudopotential-model computations of the shear-moduli ratios in compression.

IV. SUMMARY AND CONCLUSIONS

This paper includes the following results.

Formulas were derived for computing the pressure, the bulk modulus κ, and the shear moduli μ and μ' for hydrostatically loaded cubic crystals in which the atomic binding is described by a pseudopotential model. (Previously, Milstein and Hill[1,2] presented formulas for computing these moduli, but for atomic binding consisting of pairwise interaction energies ϕ depending only on current separation between the atoms; their formulas had not appeared in the subsequent literature.) The derivations of the present formulas, which are considerably more complex than those of Milstein and Hill, made use of their relations between the bulk and shear moduli, κ, μ, and μ', and the M-moduli C_{ij} under hydrostatic loading.[3,4]

A two-parameter pseudopotential model was selected for the alkali metals, and the numerical values of the two parameters were determined for each metal (Li, Na, K, Rb, Cs) by (i) matching the theoretical and experimental lattice parameters and (ii) obtaining a best least-squares fit between the theoretical and experimental values of the three zero-pressure elastic moduli (atmospheric and zero pressure are taken as synonomous here). The model employs the Heine-Abarenkov local model potential[5] and the Taylor approximation[6] for electron correlation and exchange.

The binding energies and the first and second derivatives (with respect to pressure) of the elastic moduli κ, μ, and μ' were calculated at zero pressure (as, of course, were the lattice parameters and three elastic moduli); the computed values are in very good agreement with the respective experimental values (which were available for all but the second derivatives of the shear moduli). In contrast with results based on semiempirical models (e.g., Morse,[7] Lennard-Jones,[8] Rydberg[9]) or empirical models (e.g., Johnson[10] and Baskes and Melius[11]) often used in crystal behavior studies, the accurate calculation of at least nine distinct material properties using only two empirical parameters is remarkable. In addition, we obtain excellent agreement between theoretical and experimental pressure-volume relations.

The pseudopotential model was used to determine the elastic moduli κ, μ, and μ' (as well as the pressure and binding energy) for each of the alkali metals in its bcc structure over wide ranges of hydrostatic deformation, and patterns in the observed behavior were characterized in terms of the elements' positions in the periodic table. For example, over wide ranges of pressures, at a given value of stretch, Li is the "stiffist" and Cs is the "softest," irrespective of which modulus (κ, μ, or μ') is used to characterize "stiffness" or "softness".

Comparisons were made between the general elastic

behavior of the bcc alkali metals under pressure, as described by the pseudopotential model, and that described by *any* model in which atomic binding occurs solely by pairwise central forces between atoms. For the latter, the well-known Cauchy condition ($C_{12}=C_{44}$, for the elastic constants for unstressed cubic crystals) can be generalized to $\kappa-\frac{2}{3}\mu=\mu'+2P$, for cubic crystals under hydrostatic load, as shown by Milstein and Hill.[2] This relation conveniently allowed us to identify the regions of deformation over which the elastic behavior could, in principle, be matched by a central potential model. Specific comparisons were also made among the Morse-function and pseudopotential model computations. When compared with the pseudopotential computations, the Morse function gives good representations to the pressures and bulk moduli over wide ranges of pressures, and to the shear moduli near $\lambda=1$, but important divergences occur in the shear moduli at large pressures (i.e., where instabilities occur).

In a subsequent paper, (a) the bcc computations are extended to magnitudes of compression and dilatation where lattice stability or cohesion is lost; (b) the pressures and elastic moduli are computed for the alkali metals in the fcc crystal structure over the full range of compression and expansion; (c) the domains of elastic stability are determined for each metal in both the bcc and fcc configurations; (d) special attention is focused upon the points of instability, and for each element in each crystal structure, identifications are made of the specific modes of deformation by which the (previously) stable cubic crystal transforms to the noncubic structure at the onset of each instability; (e) differences in Gibbs free energy between the fcc and bcc structures are computed over wide ranges of pressure; (f) the Gibbs free-energy and elastic stability computations are used to make predictions of phase stability and correlations with experimental results.

APPENDIX: COMPUTATIONAL TECHNIQUES AND FORMULAS

Homogeneous strains of a crystal lattice can be specified by any six parameters, q_r ($r=1,\ldots,6$), which define the geometry of a deformed cell. Elastic moduli C_{rs} can then be defined as

$$C_{rs}=1/\Omega_0(\partial^2 E_{\text{bind}}/\partial q_r \partial q_s)\ ;$$

the C_{rs} are dependent upon both the level of strain and the choice of geometric parameters q_r. Hill and Milstein[4] derived expressions relating the pressure P and moduli κ, μ, and μ' to the moduli C_{rs} for different sets of parameters q_r [see also Ref. 3, Eqs. (6.12), (6.13), and (6.14), which give these relations for the "Green," "stretch," and "M" moduli, respectively]. For computational purposes, it is convenient to define a set of moduli as

$$C_{ij}=\frac{\alpha_i\alpha_j}{\Omega}\frac{\partial^2 E_{\text{bind}}}{\partial a_i \partial a_j}\ , \tag{A1}$$

where a_1, a_2, and a_3 are the cell edges and a_4, a_5, and a_6 are their included angles; $\alpha_i=a_i$ if $i=1,2,3$ and $\alpha_i=1$ if $i=4,5,6$. With this definition, for a cubic crystal under arbitrary pressure,

$$\begin{aligned}\kappa&=\tfrac{1}{3}(C_{11}+2C_{12}+2P)\ ,\\ \mu&=\tfrac{1}{2}(C_{11}-C_{12}-P)\ ,\\ \mu'&=C_{44}-P\ .\end{aligned} \tag{A2}$$

Equations (A2) are equivalent to Eqs. (44) in Ref. 4, and the moduli C_{ij} are equivalent to the M moduli, as defined therein; introduction of the coefficient $\alpha_i\alpha_j/\Omega$ in Eq. (A1) eliminates the factor λ that appears in Eqs. (44) in Ref. 4. [Note that the C_{ij} defined by Eq. (A1) are identical to the Green moduli of Eq. (3b) at zero pressure, but differ under nonzero pressure, as is readily seen by comparing Eqs. (A2) and (3b)]. The stress components that act on the faces of the crystal cell can be written as

$$\sigma_i=\frac{\alpha_i}{\Omega}\frac{\partial E_{\text{bind}}}{\partial a_i}\ , \tag{A3}$$

where the a_i and α_i are as defined above. Equation (A3) applies to an orthorhombic (as well as cubic) crystal cell; for $i=1,2,3$, the σ_i are normal stresses acting parallel to the ith cell edge and for $i=4,5,6$ the σ_i are shear stresses. (The shear stresses are zero, but their derivatives, taken with respect to their "shearing angle," e.g., $\partial\sigma_4/\partial a_4$, are not.) For hydrostatic loading, $a_1=a_2=a_3$ and $\sigma_1=\sigma_2=\sigma_3=-P$. The procedure that we employed was to compute the elastic moduli C_{11}, C_{12}, and C_{44} and the pressure using Eqs. (A1) and (A3) and then to substitute these quantities into Eqs. (A2) to obtain κ, μ, and μ'. In order to carry out the computations, we derived analytical expressions for the pressure and C_{ij} as functions of lattice parameters a_1, a_2, and a_3; because we intend to carry out future computations for cases of nonhydrostatic loading, the derivations and final expressions are applicable to orthorhombic crystal structures (which, of course, reduce to cubic when $a_1=a_2=a_3$). Since the analytical expressions (which are derived in the following paragraphs) tend to be long and complicated, we considered it important also to do "numerical checks" using standard relations for numerical derivatives, viz.

$$\frac{\partial E_{\text{bind}}}{\partial a_i}\approx\frac{E_{\text{bind}}(a_i+\Delta a_i)-E_{\text{bind}}(a_i-\Delta a_i)}{2\Delta a_i}\ , \tag{A4}$$

and analogous expressions for $\partial^2 E_{\text{bind}}/\partial a_i\partial a_j$. With high-precision computation, Δa_i was made small enough to obtain numerical accuracy to within six to ten significant figures. Although this method of numerical differentiation is straightforward it has the disadvantage of very long computation times when a number of moduli are to be evaluated, and thus most of our computations were performed using the analytic expressions derived below.

The components of the pseudopotential binding energy of a crystal can be arranged as[5]

$$E_{\text{bind}}=E_v(\Omega)+\sum_{\mathbf{r}}E_r(\mathbf{r},\Omega)+\sum_{\mathbf{q}}E_q(\mathbf{q},\Omega)\ . \tag{A5}$$

The first term depends only on atomic volume; the summations represent real and reciprocal space summations taken over atom positions $\mathbf{r}$ and reciprocal lattice vectors $\mathbf{q}$, respectively. Both summations depend on crys-

tal structure (i.e., the geometric arrangement of the atoms and the level of strain) and also on atomic volume Ω.

The real-space part of the binding energy $E^r_{\rm bind}$ can be defined as

$$E^r_{\rm bind}=E_v(\Omega)+\sum_{\rm r}E_r(\mathbf{r},\Omega)\ . \tag{A6}$$

This part of the binding energy is a function of the atomic volume Ω and the lengths of the atom position vectors r. The derivatives of $E^r_{\rm bind}$ with respect to the a_i are

$$\frac{\partial E^r_{\rm bind}}{\partial a_i}=\frac{\partial E^r_{\rm bind}}{\partial\Omega^2}\frac{\partial\Omega^2}{\partial a_i}+\sum_{\rm r}\frac{\partial E^r_{\rm bind}}{\partial r^2}\frac{\partial r^2}{\partial a_i}\ ; \tag{A7}$$

substituting Eq. (A6) into (A7) yields

$$\frac{\partial E^r_{\rm bind}}{\partial a_i}=\frac{\partial E_v}{\partial\Omega^2}\frac{\partial\Omega^2}{\partial a_i}+\sum_{\rm r}\left[\frac{\partial E_r}{\partial\Omega^2}\frac{\partial\Omega^2}{\partial a_i}+\frac{\partial E_r}{\partial r^2}\frac{\partial r^2}{\partial a_i}\right]. \tag{A8}$$

Similarly, for the second derivative of the real-space part of the binding energy we have

$$\begin{aligned}\frac{\partial^2E^r_{\rm bind}}{\partial a_i\partial a_j}=&\frac{\partial^2E_v}{(\partial\Omega^2)^2}\frac{\partial\Omega^2}{\partial a_j}\frac{\partial\Omega^2}{\partial a_i}+\frac{\partial E_v}{\partial\Omega^2}\frac{\partial}{\partial a_j}\left[\frac{\partial\Omega^2}{\partial a_i}\right]\\&+\sum_{\rm r}\left[\frac{\partial^2E_r}{(\partial\Omega^2)^2}\frac{\partial\Omega^2}{\partial a_i}\frac{\partial\Omega^2}{\partial a_j}+\frac{\partial^2E_r}{(\partial r^2)^2}\frac{\partial r^2}{\partial a_j}\frac{\partial r^2}{\partial a_i}+\frac{\partial^2E_r}{\partial\Omega^2\partial r^2}\left[\frac{\partial\Omega^2}{\partial a_j}\frac{\partial r^2}{\partial a_i}+\frac{\partial r^2}{\partial a_j}\frac{\partial\Omega^2}{\partial a_i}\right]\right.\\&\left.+\frac{\partial E_r}{\partial\Omega^2}\frac{\partial}{\partial a_j}\left[\frac{\partial\Omega^2}{\partial a_i}\right]+\frac{\partial E_r}{\partial r^2}\frac{\partial}{\partial a_j}\left[\frac{\partial r^2}{\partial a_i}\right]\right].\end{aligned} \tag{A9}$$

Considerable simplification was obtained by writing the derivatives in terms of Ω^2 and r^2, since these quantities are conveniently related to the a_i as follows. Writing

$$\Omega=\frac{\mathbf{a}_3\cdot(\mathbf{a}_1\times\mathbf{a}_2)}{n} \tag{A10}$$

leads to

$$\Omega^2=\frac{a_1^2a_2^2a_2^2}{n}[1+2\cos a_4\cos a_5\cos a_6-\cos^2a_4-\cos^2a_5-\cos^2a_6]\ , \tag{A11}$$

where n is the number of atoms per crystal cell. For a Bravais crystal the $\mathbf{r}$ may be represented in terms of a combination of the crystal Bravais vectors $\mathbf{b}_i$ as

$$\mathbf{r}=m_1\mathbf{b}_1+m_2\mathbf{b}_2+m_3\mathbf{b}_3\ , \tag{A12}$$

where the m_i are integers. Each of the Bravais vectors may in turn be represented by a combination of the vectors $\mathbf{a}_i$ as

$$\mathbf{b}_i=B_{i1}\mathbf{a}_1+B_{i2}\mathbf{a}_2+B_{i3}\mathbf{a}_3\ , \tag{A13}$$

where the B_{ij} are constants determined by the crystal structure and the crystal cell being considered. (For a conventional fcc cell, for example, one could write $\mathbf{b}_1=\mathbf{a}_1$, $\mathbf{b}_2=0.5\mathbf{a}_1+0.5\mathbf{a}_2$, and $\mathbf{b}_3=0.5\mathbf{a}_1+0.5\mathbf{a}_3$.) Substituting Eq. (A13) into Eq. (A12) gives

$$\mathbf{r}=l_1\mathbf{a}_1+l_2\mathbf{a}_2+l_3\mathbf{a}_3\ , \tag{A14}$$

where

$$l_i=\sum_j m_jB_{ji}\ . \tag{A15}$$

(The convention used in this section for summations over indices is that each index runs over the values 1, 2, and 3.) Then

$$r^2=\sum_{i,j}l_il_ja_ia_j\cos(a_{i,j})\ , \tag{A16}$$

where $a_{i,j}$ is the angle between $\mathbf{a}_i$ and $\mathbf{a}_j$ (for example, for $i=j$, $a_{i,j}=0$, and for $i=1$ and $j=2$, $a_{i,j}=a_6$). The derivatives of Ω^2 and r^2 with respect to the a_i are found from Eqs. (A11) and (A16):

$$\begin{aligned}&\frac{\partial\Omega^2}{\partial a_i}=\frac{2\Omega^2}{a_i},\quad\frac{\partial r^2}{\partial a_i}=2l_i^2a_i\ ,\\&\frac{\partial}{\partial a_1}\left[\frac{\partial\Omega^2}{\partial a_1}\right]=\frac{2\Omega^2}{a_1^2},\quad\frac{\partial}{\partial a_1}\left[\frac{\partial r^2}{\partial a_1}\right]=2l_1^2\ ,\\&\frac{\partial}{\partial a_2}\left[\frac{\partial\Omega^2}{\partial a_1}\right]=\frac{4\Omega^2}{a_1a_2},\quad\frac{\partial}{\partial a_2}\left[\frac{\partial r^2}{\partial a_1}\right]=0\ ,\\&\frac{\partial\Omega^2}{\partial a_4}=0,\quad\frac{\partial}{\partial a_4}\left[\frac{\partial\Omega^2}{\partial a_4}\right]=-2\Omega^2\ ,\\&\frac{\partial r^2}{\partial a_4}=-2l_2l_3a_2a_3,\quad\frac{\partial}{\partial a_4}\left[\frac{\partial r^2}{\partial a_4}\right]=0\ .\end{aligned} \tag{A17}$$

Consider the real-space contribution σ^r_i to the normal stress σ_i,

$$\sigma^r_i=\frac{a_i}{\Omega}\frac{\partial E^r_{\rm bind}}{\partial a_i},\quad i=1,2,3 \tag{A18}$$

substituting Eq. (A8) and the first two equations of (A17) into (A18) yields, after simplification,

$$\sigma^r_i=\frac{\partial E_v}{\partial\Omega}+\sum_{\rm r}\frac{\partial E_r}{\partial\Omega}+\frac{a_i^2}{\Omega}\sum_{\rm r}\frac{l_i^2}{r}\frac{\partial E_r}{\partial r}\ . \tag{A19}$$

The real-space contributions C^r_{11}, C^r_{12}, and C^r_{44} to the moduli C_{11}, C_{12}, and C_{44}, respectively, are [from Eq. (A1)]

$$C^r_{11}=\frac{a_1^2}{\Omega}\frac{\partial^2 E^r_{\rm bind}}{(\partial a_1)^2},\quad C^r_{12}=\frac{a_1a_2}{\Omega}\frac{\partial^2 E^r_{\rm bind}}{\partial a_1\partial a_2},\quad C^r_{44}=\frac{1}{\Omega}\frac{\partial^2 E^r_{\rm bind}}{(\partial a_4)^2}\ , \tag{A20}$$

substituting Eq. (A9) and the appropriate equations of (A17) into (A20) yields, after simplification

$$C^r_{11}=\Omega\frac{\partial^2 E_v}{\partial\Omega^2}+\Omega\sum_{\rm r}\frac{\partial^2 E_r}{\partial\Omega^2}+\frac{a_1^2}{\Omega}\sum_{\rm r}\frac{l_1^2}{r}\frac{\partial E_r}{\partial r}+2a_1^2\sum_{\rm r}\frac{l_1^2}{r}\frac{\partial^2 E_r}{\partial\Omega\partial r}+\frac{a_1^4}{\Omega}\sum_{\rm r}\frac{l_1^4}{r^2}\left[\frac{-1}{r}\frac{\partial E_r}{\partial r}+\frac{\partial^2 E_r}{\partial r^2}\right],$$

$$C^r_{12}=\frac{\partial E_v}{\partial\Omega}+\Omega\frac{\partial^2 E_v}{\partial\Omega^2}+\sum_{\rm r}\frac{\partial E_r}{\partial\Omega}+\Omega\sum_{\rm r}\frac{\partial^2 E_r}{\partial\Omega^2}+\sum_{\rm r}(a_1^2l_1^2+a_2^2l_2^2)\frac{1}{r}\frac{\partial^2 E_r}{\partial\Omega\partial r}+\frac{a_1^2a_2^2}{\Omega}\sum_{\rm r}\frac{l_1^2l_2^2}{r^2}\left[\frac{-1}{r}\frac{\partial E_r}{\partial r}+\frac{\partial^2 E_r}{\partial r^2}\right], \tag{A21}$$

$$C^r_{44}=-\frac{\partial E_v}{\partial\Omega}-\sum_{\rm r}\frac{\partial E_r}{\partial\Omega}+\frac{a_2^2a_3^2}{\Omega}\sum_{\rm r}\frac{l_2^2l_3^2}{r^2}\left[\frac{-1}{r}\frac{\partial E_r}{\partial r}+\frac{\partial^2 E_r}{\partial r^2}\right].$$

Equations (A19) and (A21) thus give the analytic form for the real-space contributions to the normal stresses and elastic constants; we now develop equations for the reciprocal-space contributions σ_i^q and C_{ij}^q, where $\sigma_i=\sigma_i^r+\sigma_i^q$ and $C_{ij}=C_{ij}^r+C_{ij}^q$. The reciprocal-space part of the binding energy is

$$E^q_{\rm bind}=\sum_{\mathbf{q}}E_q(\mathbf{q},\Omega)\ , \tag{A22}$$

and the expressions defining σ_i^q and C_{ij}^q are the same as Eqs. (A18) and (A20) except that the superscript q replaces the superscript r. Also, the derivatives of $E^q_{\rm bind}$ with respect to the a_i are the same as Eqs. (A8) and (A9), but with E_v and its derivatives $=0$ and with r replaced by q throughout. Once the derivatives of q^2 with respect to the a_i have been determined, explicit equations for the σ_i^q and the C_{ij}^q can be written. The relations between q^2 and the a_i (which are more complicated than those between the r^2 and the a_i) are developed as follows.

Reciprocal-lattice vectors $\mathbf{q}$ are defined by

$$\mathbf{q}=n_1\mathbf{p}_1+n_2\mathbf{p}_2+n_3\mathbf{p}_3\ , \tag{A23}$$

where the n_i are integers and $\mathbf{p}_i$ are given by

$$\mathbf{p}_1=\frac{2\pi}{\Omega}\mathbf{b}_2\times\mathbf{b}_3,\quad \mathbf{p}_2=\frac{2\pi}{\Omega}\mathbf{b}_3\times\mathbf{b}_1,\quad \mathbf{p}_3=\frac{2\pi}{\Omega}\mathbf{b}_1\times\mathbf{b}_2\ , \tag{A24}$$

and the $\mathbf{b}_i$ are the crystal Bravais vectors defined by Eq. (A13). From Eq. (A23),

$$q^2=\sum_{i,j}n_in_j(\mathbf{p}_i\cdot\mathbf{p}_j)\ . \tag{A25}$$

Consider the quantity

$$\mathbf{p}_1\cdot\mathbf{p}_2=\frac{4\pi^2}{\Omega^2}(\mathbf{b}_2\times\mathbf{b}_3)\cdot(\mathbf{b}_3\times\mathbf{b}_1)\ ,$$

which may be rewritten as

$$\mathbf{p}_1\cdot\mathbf{p}_2=\frac{4\pi^2}{\Omega^2}[(\mathbf{b}_2\cdot\mathbf{b}_3)(\mathbf{b}_1\cdot\mathbf{b}_3)-(\mathbf{b}_3\cdot\mathbf{b}_3)(\mathbf{b}_1\cdot\mathbf{b}_2)]\ . \tag{A26}$$

If each of the $\mathbf{p}_i\cdot\mathbf{p}_j$ terms in Eq. (A25) is replaced by a similar expression, we obtain

$$q^2=\frac{4\pi^2}{\Omega^2}\sum_{i,j,k}\left[\frac{\varepsilon^+_{ijk}}{2}n_i^2[(\mathbf{b}_j\cdot\mathbf{b}_j)(\mathbf{b}_k\cdot\mathbf{b}_k)-(\mathbf{b}_j\cdot\mathbf{b}_k)^2]+\varepsilon^+_{ijk}n_in_j[(\mathbf{b}_j\cdot\mathbf{b}_k)(\mathbf{b}_i\cdot\mathbf{b}_k)-(\mathbf{b}_k\cdot\mathbf{b}_k)(\mathbf{b}_i\cdot\mathbf{b}_j)]\right], \tag{A27}$$

where

$$\varepsilon^+_{ijk}=\begin{cases}0 & \text{if } i=j \text{ or } j=k \text{ or } i=k\ ,\\ 1 & \text{if } i\neq j \text{ and } j\neq k \text{ and } i\neq k\ .\end{cases} \tag{A28}$$

From Eq. (A13),

$$\mathbf{b}_i\cdot\mathbf{b}_j=\sum_{t,u}B_{it}B_{ju}a_ta_u\cos(a_{t,u})\ ;$$

substituting this into Eq. (A27) and simplifying yields

$$q^2=\frac{4\pi^2}{\Omega^2}\sum_{t,u,v,w}[a_ta_u\cos(a_{t,u})a_va_w\cos(a_{v,w})K_{tuvw}]\ , \tag{A29}$$

where

$$K_{tuvw}=\sum_{i,j,k}\left[\varepsilon^+_{ijk}\left[\frac{n_i^2}{2}(B_{jt}B_{ju}B_{kv}B_{kw}-B_{jt}B_{ku}B_{jv}B_{kw})+n_in_j(B_{jt}B_{ku}B_{iv}B_{kw}-B_{kt}B_{ku}B_{iv}B_{jw})\right]\right]. \tag{A30}$$

It can be seen from Eq. (A30) that $K_{tuvw}=0$ when $t=u=v=w$. Also for an orthorhombic crystal cell $\mathbf{a}_t\cdot\mathbf{a}_u=0$ when $t\neq u$, and $\mathbf{a}_v\cdot\mathbf{a}_w=0$ when $v\neq w$; this significantly reduces the number of terms in Eq. (A29). In particular, for an orthorhombic crystal cell,

$$q^2=\frac{4\pi^2}{\Omega^2}[a_1^2a_2^2(K_{1122}+K_{2211})+a_1^2a_3^2(K_{1133}+K_{3311})+a_2^2a_3^2(K_{2233}+K_{3322})]\ . \tag{A31}$$

The derivatives of q^2 with respect to the a_i for values of i of 1,2, or 3 are, from Eq. (A31),

$$\frac{\partial q^2}{\partial a_i}=-\frac{8\pi^2a_j^2a_k^2}{\Omega^2a_i}(K_{jjkk}+K_{kkjj})\ , \tag{A32}$$

where i,j,k=any order of 1, 2, 3, and

$$\frac{\partial}{\partial a_1}\left[\frac{\partial q^2}{\partial a_1}\right]=\frac{24\pi^2 a_2^2 a_3^2}{\Omega^2 a_1^2}(K_{2233}+K_{3322}),\quad \frac{\partial}{\partial a_2}\left[\frac{\partial q^2}{\partial a_1}\right]=0\ . \tag{A33}$$

For $i=4$, 5, or 6, the more general expression, Eq. (A29), must be used because, in taking these derivatives, the crystal cell is "sheared away from" the orthorhombic structure. The results for $i=4$ are

$$\frac{\partial q^2}{\partial a_4}=-\frac{4\pi^2}{\Omega^2}a_2a_3[a_1^2(K_{1123}+K_{1132}+K_{2311}+K_{3211})$$
$$+a_2^2(K_{2223}+K_{2232}+K_{2322}+K_{3222})+a_3^2(K_{3323}+K_{3332}+K_{2333}+K_{3233})]\ , \tag{A34}$$

$$\frac{\partial}{\partial a_4}\left[\frac{\partial q^2}{\partial a_4}\right]=\frac{8\pi^2}{\Omega^2}[a_1^2a_2^2(K_{1122}+K_{2211})+a_1^2a_3^2(K_{1133}+K_{3311})$$
$$+a_2^2a_3^2(K_{2233}+K_{3322})+a_2^2a_3^2(K_{2323}+K_{2332}+K_{3223}+K_{3232})]\ . \tag{A35}$$

Finally, we substitute Eqs. (A32)—(A35) into the equations that are the reciprocal-space analogs of Eqs. (A8) and (A9) which are then substituted into the reciprocal-space analogs of Eqs. (A18) and (A20). This procedure yields

$$\sigma_i^q=-\frac{4\pi^2}{\Omega^3}a_j^2a_k^2\sum_{\mathbf{q}}\frac{(K_{jjkk}+K_{kkjj})}{q}\frac{\partial E_q}{\partial q} \tag{A36}$$

for the reciprocal-space part of the normal stresses, where $i,j,k=$any order of 1, 2, 3. For the reciprocal-space part of the elastic constants,

$$C_{11}^q=\frac{12\pi^2a_2^2a_3^2}{\Omega^3}\sum_{\mathbf{q}}\frac{(K_{2233}+K_{3322})}{q}\frac{\partial E_q}{\partial q}$$
$$+\frac{16\pi^4a_2^4a_3^4}{\Omega^5}\sum_{\mathbf{q}}\frac{(K_{2233}+K_{3322})^2}{q^2}\left[\frac{-1}{q}\frac{\partial E_q}{\partial q}+\frac{\partial^2E_q}{\partial q^2}\right]-\frac{8\pi^2a_2^2a_3^2}{\Omega^2}\sum_{\mathbf{q}}\frac{(K_{2233}+K_{3322})}{q}\frac{\partial^2E_q}{\partial\Omega\partial q}\ ,$$
$$C_{12}^q=\frac{-4\pi^2a_2^2a_3^2}{\Omega^2}\sum_{\mathbf{q}}\frac{(K_{2233}+K_{3322})}{q}\frac{\partial^2E_q}{\partial\Omega\partial q}-\frac{4\pi^2a_1^2a_3^2}{\Omega^2}\sum_{\mathbf{q}}\frac{(K_{1133}+K_{3311})}{q}\frac{\partial^2E_q}{\partial\Omega\partial q}$$
$$+\frac{16\pi^4a_1^2a_2^2a_3^4}{\Omega^5}\sum_{\mathbf{q}}\frac{(K_{2233}+K_{3322})(K_{1133}+K_{3311})}{q^2}\left[\frac{-1}{q}\frac{\partial E_q}{\partial q}+\frac{\partial^2E_q}{\partial q^2}\right]\ ,$$
$$C_{44}^q=\frac{4\pi^2}{\Omega^3}\sum_{\mathbf{q}}\frac{1}{q}\frac{\partial E_q}{\partial q}[a_1^2a_2^2(K_{1122}+K_{2211})+a_1^2a_3^2(K_{1133}+K_{3311}) \tag{A37}$$
$$+a_2^2a_3^2(K_{2233}+K_{3322})+a_2^2a_3^2(K_{2323}+K_{2332}+K_{3223}+K_{3232})]$$
$$+\frac{4\pi^4a_2^2a_3^2}{\Omega^5}\sum_{\mathbf{q}}\frac{1}{q^2}\left[\frac{-1}{q}\frac{\partial E_q}{\partial q}+\frac{\partial^2E_q}{\partial q^2}\right][a_1^2(K_{1123}+K_{1132}+K_{2311}+K_{3211})$$
$$+a_2^2(K_{2223}+K_{2232}+K_{2322}+K_{3222})$$
$$+a_3^2(K_{3323}+K_{3332}+K_{2333}+K_{3233})]^2\ .$$

The total normal stress $\sigma_i=\sigma_i^r+\sigma_i^q$ ($=-P$ for a cubic crystal) is then computed from Eqs. (A19) and (A36) and the elastic moduli $C_{ij}=C_{ij}^r+C_{ij}^q$ are computed from Eqs. (A21) and (A37). The real-space lattice sum is over values of r determined from Eq. (A16) and the values of q in the reciprocal-space sum are computed from Eq. (A31). The lattice-summation technique is described in detail in Ref. 35.

ACKNOWLEDGMENTS

This work was supported by the National Science Foundation under Grant No. DMR-81-06022. This work is based upon parts of the Ph.D. Dissertation of D. J. Rasky, University of California, Santa Barbara.

*Present address: Acurex Corporation, 555 Clyde Ave., Mountain View, CA 94042.
[1]F. Milstein and R. Hill, J. Mech. Phys. Solids **25**, 457 (1977).
[2]F. Milstein and R. Hill, J. Mech. Phys. Solids **26**, 213 (1978).
[3]F. Milstein and R. Hill, J. Mech. Phys. Solids **27**, 255 (1979).
[4]R. Hill and F. Milstein, Phys. Rev. B **15**, 3087 (1977).
[5]V. Heine and D. Weaire, in *Solid State Physics*, edited by H. Ehrenreich, F. Seitz, and D. Turnbull (Academic, New York, 1970), Vol. 24.
[6]R. Taylor, J. Phys. F **8**, 1699 (1978).
[7]P. M. Morse, Phys. Rev. **34**, 57 (1929).
[8]J. E. Lennard-Jones, Proc. R. Soc. London Sect. A **106**, 463 (1924).
[9]R. Rydberg, Z. Phys. **73**, 376 (1931).
[10]R. A. Johnson, J. Phys. F **3**, 295 (1973).
[11]M. I. Baskes and C. F. Melius, Phys. Rev. B **20**, 3197 (1979).
[12]F. Milstein and R. Hill, Phys. Rev. Lett. **43**, 1411 (1979).
[13]D. Sen and S. K. Sarkar, Phys. Rev. B **22**, 1856 (1979).
[14]T. Soma, Physica **97B**, 76 (1979).
[15]S. Benckert, Phys. Status Solidi B **69**, 483 (1975).
[16]E. G. Brovman and Y. M. Kagan, Usp. Fiz. Nauk **112-114**, 369 (1974) [Sov. Phys.—Usp. **17**, 125 (1975)].
[17]K. Shimada, Phys. Status Solidi B **61**, 325 (1974).
[18]D. C. Wallace, Phys. Rev. **178**, 900 (1969).
[19]T. Suzuki, A. V. Granato, and J. F. Thomas, Phys. Rev. **175**, 766 (1969).
[20]R. W. Shaw, Jr., J. Phys. C **2**, 2335 (1969).
[21]R. Pick, J. Phys. (Paris) **28**, 539 (1967).
[22]W. A. Harrison, Phys. Rev. **136**, 1107 (1963).
[23]T. Suzuki and H. M. Ledbetter, Philos. Mag. A **48**, 83 (1983).
[24]J. Eftis, D. E. MacDonald, and G. M. Arkilic, Mater. Sci. Eng. **7**, 141 (1971).
[25]N. W. Ashcroft, Phys. Lett. **23**, 48 (1966).
[26]M. Born, Proc. Cambridge Philos. Soc. **36**, 160 (1940).
[27]M. Born and R. Fürth, Proc. Cambridge Philos. Soc. **36**, 454 (1940).
[28]R. Fürth, Proc. Cambridge Philos. Soc. **37**, 177 (1941).
[29]R. Hill, J. Mech. Phys. Solids **16**, 229 (1968).
[30]R. Hill, Math. Proc. Cambridge Philos. Soc. **77**, 225 (1975).
[31]N. H. Macmillan and A. Kelly, Proc. R. Soc. London Sect. A **330**, 309 (1972).
[32]D. C. Wallace, *Thermodynamics of Crystals* (Wiley, New York, 1972).
[33]F. Milstein and B. Farber, Philos. Mag. A **42**, 19 (1980).
[34]F. Milstein and D. J. Rasky, Philos. Mag. A **45**, 49 (1982).
[35]D. J. Rasky and F. Milstein, in *Continuum Models of Discrete Systems 4*, edited by O. Brulin and R. K. T. Hsieh (North-Holland, Amsterdam, 1981), p. 265.
[36]G. C. Kennedy and R. N. Keeler, in *American Institute of Physics Handbook*, edited by D. E. Gray (McGraw-Hill, New York, 1972), Chap. 4d.
[37]W. A. Harrison, *Pseudopotentials in the Theory of Metals* (Benjamin, New York, 1966).
[38]C. A. Swenson, J. Phys. Chem. Solids **27**, 33 (1966).
[39]F. Milstein, J. Appl. Phys. **44**, 3825 (1973).
[40]G. Simmons and H. Wang, *Temperature Variation of Elastic Constants and Calculated Aggregate Properties* (MIT Press, Cambridge, Mass., 1971).